Lasers in Manufacturing Conference 2017

Application specific intensity distributions for laser functionalization of (nano-)ceramic coatings as wear protection

Annika Völl[a*], Susanne Wollgarten[a], Jochen Stollenwerk[a, b], Peter Loosen[a,b]

[a]*Chair for Technology of Optical Systems, RWTH Aachen University, Steinbachstraße 15, 52074 Aachen, Germany*
[b]*Fraunhofer Institute for Laser Technology, Steinbachstraße 15, 52074 Aachen, Germany*

Abstract

The laser based functionalization of thin sol-gel based (nano-)ceramic coatings requires a two-step thermal process. First, the solvent material, in which the ceramic is applied, needs to be removed in a drying process. Afterwards, during a second step that removes the last organic constituents, the ceramic's full potential as wear protection coating is achieved via cross-linking. As both steps require significantly different processing temperatures, the material usually is treated in two consecutive laser based processes. Thus, the process efficiency can be increased to a great extent by using application specific beam profiles. These beam profiles can be designed in such a way that they combine both steps into a single one by raising the induced material temperature stepwise. To this end, we present a method to obtain an application specific intensity distribution that induces a prescribed temperature profile in a layered system consisting of a metal substrate and a thin (nano-)ceramic coating. This is done by solving an inverse heat conduction problem using the conjugate gradient approach with adjoint problem. Afterwards, we give the design of a free-form optic that produces the obtained intensity distribution in an experimental setup. We conclude our work by verifying our approach using the commercial FEM software ANSYS.

Keywords: Surface Functionalization; Process Simulation;

1. Introduction

To increase the lifetime of hardly stressed machine components, it has become state-of-the-art to coat the components in question with a thin wear protective film (Bach et al., 2005, Hieke, 2000, Mellor 2006). While possible coating materials range from metallic to ceramic thin films, one frequently applied method for the placement of ceramic thin films is the usage of sol-gels (Dislich, 1988). This process strategy has the advantage that it is much less complicated than other commonly used deposition methods such as PVD or CVD. In sol-gels, a preliminary stage of the ceramic is mixed with a fluid solvent in which it is deposited on

* *Corresponding author. Tel.: +49 241 8906 8369; fax: +49 241 8906 121.*
E-mail address: annika.voell@tos.rwth-aachen.de.

the processed surface. To form the final state of the ceramic, an additional functionalizing step is necessary in which the finishing chemical reactions take place.

Therefore, the production of a thin wear protective sol-gel based (nano-)ceramic coating is a three-step process. First, the sol-gel needs to be deposited on the substrate's surface. Here, several methods as e.g. dip coating or spin coating are used. Afterwards, the solvent material must be removed in a drying step. In this thermal treatment, lower temperatures (<500 °C) are necessary. Finally, the aforementioned functionalizing step takes place at higher temperatures (>800 °C). Usually, the two thermal treatment steps are performed in oven-based processes (Uhlmann et al., 2013). However, it can be shown that these steps can also be conducted in laser-based thermal treatments resulting in a much more efficient process (Hawelka, 2015).

Because of the two different temperature ranges for the drying step on one hand and the functionalizing step on the other, no combination of those treatments in a single laser-based processing step has been performed up to now. To this end, special beam shaping methods offer a great potential.

In our previous work (Völl et al., 2016), a strategy for beam shaping in laser heat treatment applications has been presented that calculates a specific intensity distribution which induces a prescribed temperature profile within the material. This numerical method is based on solving an inverse heat conduction problem for the thermal treatment. To do so, the heat conduction equation is solved iteratively using the conjugate gradient method with adjoint problem (Alifanov, 1994, Özisik and Orlande, 2000). In Stollenwerk et al., 2015, we also present an idea of how to create the resulting, very inhomogeneous intensity distributions. Hence, one method might be the usage of free-form optics that can create nearly arbitrary intensity distributions because of the possibility to adapt many degrees of freedom.

In the following, we present the necessary temperature-time sequence that combines the drying and the functionalizing steps of a laser-based process to create a (nano-)ceramic coating as wear protection. Using our strategy for deriving an application specific intensity distribution, we will derive a corresponding intensity distribution that induces the derived temperature profile within the material. Finally, we will present a design for a free-form optic that creates the calculated intensity distribution on the workpiece's surface. We will furthermore verify our results using the commercial FEM-software ANSYS.

2. Material & Simulation Method

2.1. Material properties

Our goal is to create a (nano-)ceramic sol-gel based coating of $Zr0_2$ (Uhlmann et al., 2013) on a plane 100Cr6 steel (Spittel and Spittel, 2009) substrate. It has been shown that this coating can be used as a protective layer on the steel surface by increasing the component's hardness on that surface (Uhlmann et al., 2013). We assume that the coating has been deposited on the surface of the material by dip coating which should result in a layer thickness of about 100 nm (Hawelka, 2015). As the thermal conductivity of the ZrO_2 solution is very low and because of this comparable small thickness of the layer, we assume that its temperature is identical with the surface temperature of the substrate material. Furthermore, the solution is transparent at the wavelength of the laser beam. Thus, we assume that the coating is heated over the substrate. With this reasoning, we will neglect the coating in the following temperature simulations to increase the numerical efficiency.

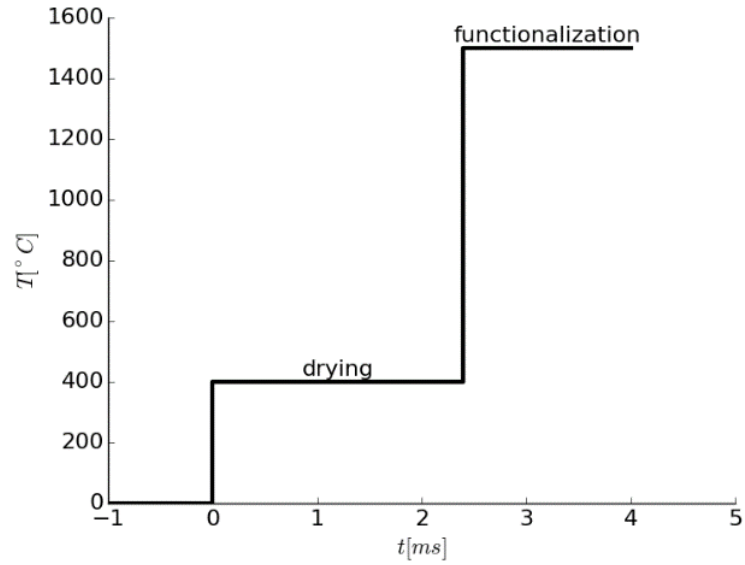

Fig. 1. Temperature – time sequence to combine the drying step and the functionalization step in a process to create sol-gel based (nano-) ceramic coatings as wear protection.

The general feasibility of a laser-based functionalizing of a ZrO_2 – Sol-Gel on the steel 100Cr6 has been shown in Hawelka, 2015. Furthermore, it is possible to derive the optimal processing temperature profile from this work. According to Hawelka, the following temperature-time sequences are ideal:

- Drying process: 400 °C for 2.4 ms
- Functionalizing step: 1 500 °C for 1.6 ms

This can be combined in a single-step process as shown in Fig. 1. First, the temperature is held at 400°C for 2.4 ms to remove the solvent material. Directly afterwards, the temperature is increased to 1 500°C to initiate the necessary chemical reactions that create the functionalized (nano-)ceramic coating. As we assume that we process the material at a constant feed speed $\vec{v}$, this can be transformed in a temperature-space curve via $\vec{s} = \vec{v}t$. We aim to induce this temperature-space profile in the treated material.

2.2. Solution of the inverse heat conduction problem

In the following, we will summarize the results from Völl et al., 2016 in order to present a method to derive the application specific intensity distribution for a prescribed temperature profile. This problem is known to be ill-posed and special regularization methods are necessary (Beck et al., 1985).

We assume that the laser beam is moving at constant feed speed $\vec{v}$ over the material's surface. For a given intensity distribution, the induced temperature field can be calculated using the heat conduction equation

$$-\nabla(k\nabla T) = -\vec{v}\rho c\nabla T \qquad (k\text{: thermal conductivity}, \rho\text{: density}, c\text{: specific heat}) \qquad (1)$$

with appropriate boundary conditions. For the material combination described in the previous section, the absorption of the laser beam at the steel's surface can be represented by the Neumann boundary condition

$$-k\vec{n}\nabla T = AI \qquad (\vec{n}\text{: surface normal}, A\text{: absorptance}) \tag{2}$$

Assuming, that the target temperature profile is prescribed at a given set of N points, the deviation between a given temperature field T and the prescribed field Y can be computed using the least-squares sum

$$S = \sum_i (T_i - Y_i)^2 \tag{3}$$

Based on this quantity, an iterative method for the solution of the inverse heat conduction problem can be implemented. At first, an initial guess for the intensity distribution is assumed and the corresponding temperature profile is evaluated with Eq. (1). Using the outcome, S is calculated and it is checked if the stopping criterion is met. If this is not the case, the intensity distribution I is updated via

$$I^{n+1} = I^n + \delta I^n \tag{4}$$

In the conjugate gradient method with adjoint problem, this update is given by

$$\delta I^n = -\beta^n d^n \tag{5}$$

where d^n is the combination of the steepest decent direction and the previous update direction

$$d^n = \nabla S(I^n) + \gamma^n d^{n-1} \tag{6}$$

To calculate β and γ, two additional partial differential equations need to be solved. To calculate the steepest decent direction ∇S, the adjoint problem

$$-k\nabla(\nabla\lambda) = -2(Y_i - T_i)\delta(x - x_i)\delta(y - y_i)\delta(z - z_i) - \vec{v}\left(\rho c + \rho\frac{\partial c}{\partial T}T + c\frac{\partial \rho}{\partial T}T\right)\nabla\lambda \tag{7}$$

is solved from which the steepest decent direction can be calculated via

$$\nabla S_j = \int_{\partial\Omega_j} A\lambda d\Omega \tag{8}$$

Additionally, it is necessary to calculate the temperature change for an incremental change in the intensity distribution. To this end, a sensitivity problem

$$-\nabla\big(\nabla(k\Delta T)\big) = -\vec{v}\nabla\left(\left(\rho c + \rho\frac{\partial c}{\partial T}T + c\frac{\partial \rho}{\partial T}T\right)\Delta T\right) \tag{9}$$

is solved. See Völl et al., 2016 for a more detailed description.

The main advantage of this method compared to other inverse methods is that in each iteration step only three solutions of partial differential equations are necessary. This results in a strong reduction of the computational effort.

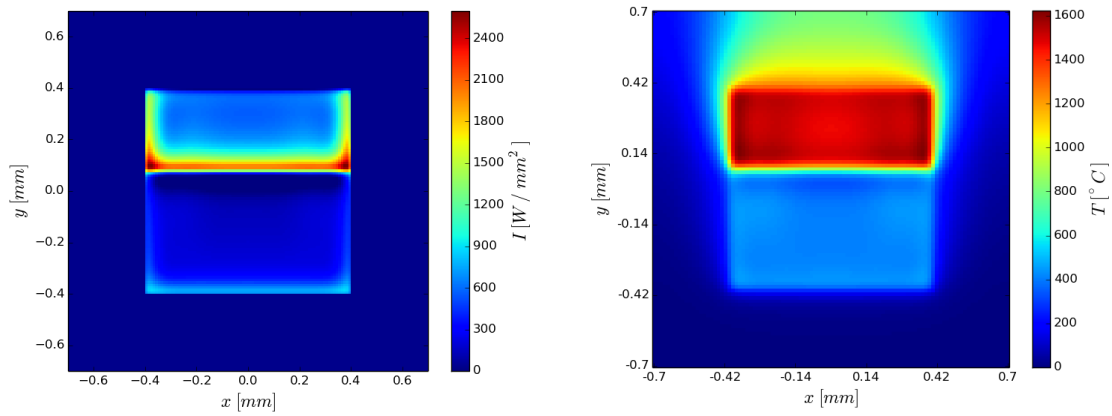

Fig. 2. Computed intensity distribution to obtain the temperature-time sequence as shown in Fig. 1. (left); Surface temperature profile obtained with the computed intensity distribution (right).

3. Numerical Results

3.1. Application specific intensity distribution

In this section, we will use the presented method to derive an intensity distribution that induces the temperature-time sequence presented in Fig. 1. Before running the simulation, it is necessary to define the process parameters. We would like to use a diode laser beam with 450 W maximum output power. This finite power is the limiting factor for the spot size and accordingly for the feed speed. This holds, as increasing the spot size by keeping the temperature holding time constant would result in an increased feed speed. To fix spot size and feed speed, we run a few simulations with lower precision and fewer iterations and compare the needed power. From this, we obtain a rectangular spot size of 0.8 mm x 0.8 mm which implies a feed speed of $\vec{v} = (0.0, 200)^T$ mm/s. As shown below, this results in a power well below 450 W.

Furthermore, we use the l-curve method (Hansen and O'Leary, 1995) to fix the number of iterations of the solution algorithm to 10. Thus, the solution is regularized in such a way that it is neither over-smoothed nor over-fitted.

Fig. 2 shows the results of the algorithm from section 2.2 for this case. On the left, the intensity distribution is presented and on the right the temperature profile is shown that is achieved on the steel's surface using this intensity distribution. In the intensity distribution, the two different processing steps are clearly visible and the shape of each step is similar. In both cases, we obtain a high intensity value at the lower edge, some elevations on the side edges and a rather small intensity value in the main area. The explanation for this is rather straightforward (see also Völl et al. 2016). In the beginning, the material needs to be heated to the prescribed temperature. For this, the high intensity is necessary. Afterwards, the temperature only needs to be kept constant. Therefore, only a smaller intensity is needed. The elevations on the sides account for the heat diffusion into the material. The total power needed to obtain this intensity distribution is 350 W.

The obtained temperature profile on the substrate's surface is very homogeneous in both steps, showing a temperature of approximately 400°C and 1 500°C respectively. Thus, we have derived an intensity distribution that can induce the prescribed temperature profile from Fig. 1.

3.2. Freeform optic design & ANSYS verification

The intensity distribution in Fig. 2 (left) is inhomogeneous and has very prominent features as e. g. thin lines and sharp edges. Therefore, it is rather challenging to create this intensity profile in an experimental setup. Here, we suggest to use free-form optics for the realization of this intensity distributions. Free-form optics have many more degrees of freedom than the commonly used spheres or aspheres. Moreover, they can be designed in such a way that nearly every illuminance pattern can be obtained on the target surface (Bruneton et al., 2013). Here, we use a state-of-the-art free-form optic design algorithm (Bäuerle et al., 2012) to obtain a free-form lens that forms the intensity distribution from Fig. 2.

The experimental setup which we assume for the free-form optic design is shown on the right in Fig. 3. The incoming (collimated) laser beam, whose cross-section intensity profile is shown in Fig. 3 (left), is formed by a free-form lens in such a way that the working distance between lens and workpiece surface amounts to 70 mm.

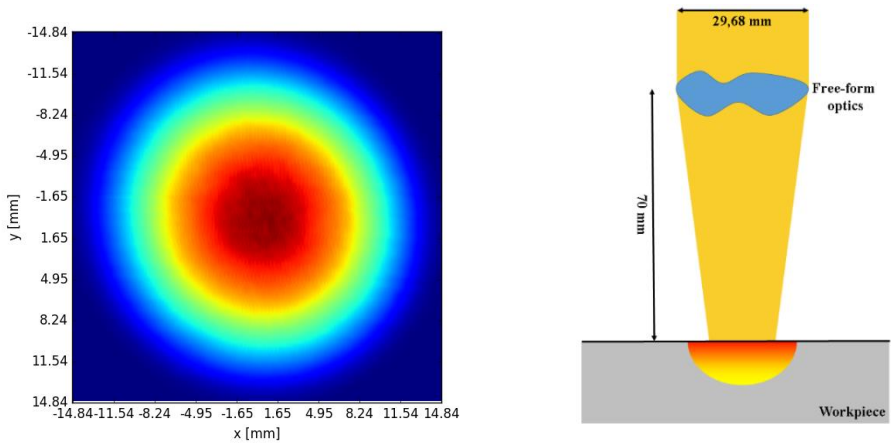

Fig. 3. Measured intensity distribution of the input laser beam (left); Sketch of the experimental setup for the free-form lens (right).

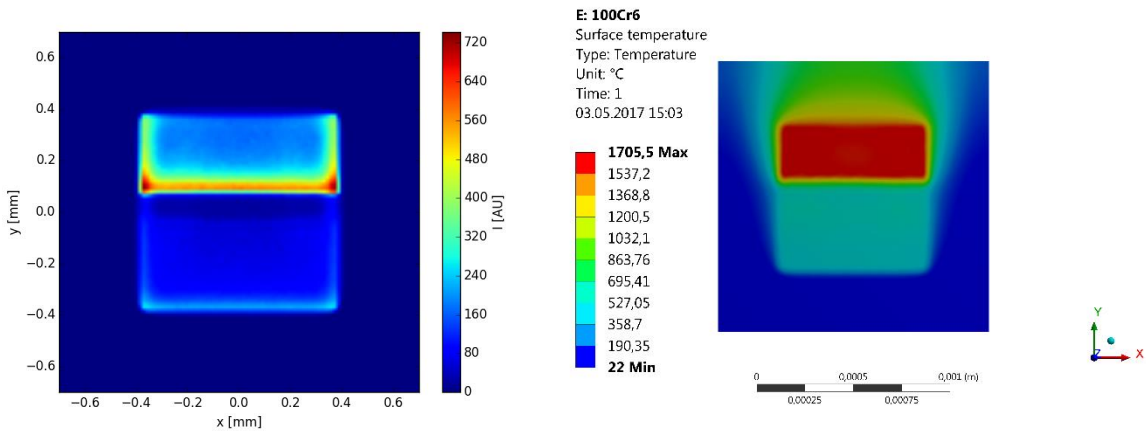

Fig. 4. Intensity distribution obtained with the designed free-form lens (ray tracing result) (left); Calculated temperature profile on the workpiece's surface using this intensity distribution (right).

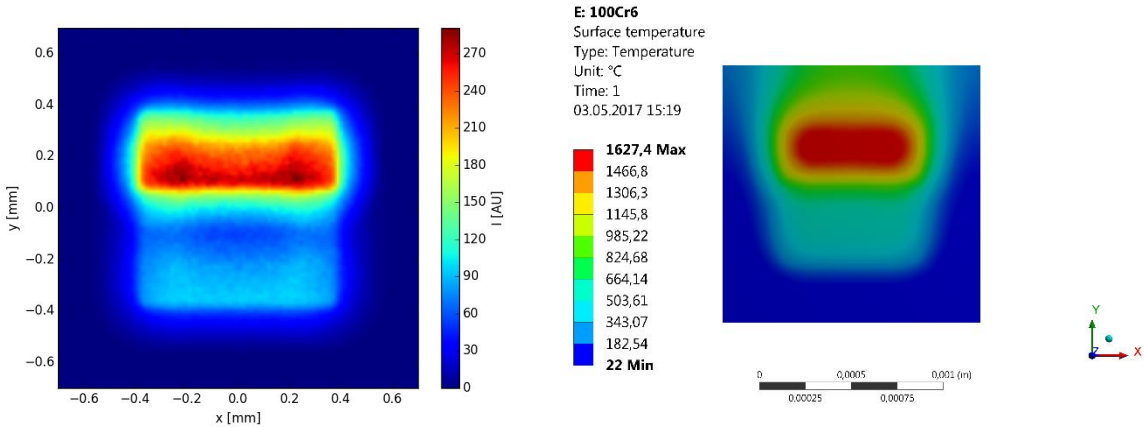

Fig. 5. Intensity distribution obtained with the designed free-form lens respecting the finite divergence angle of the incoming laser beam (ray-tracing result) (left); Calculated temperature profile on the workpiece's surface using this intensity distribution (right).

The result for the obtained intensity pattern is shown in Fig. 4 (left). It is obvious that the calculated intensity profile from Fig. 2 and this result are in good agreement. Subsequently, the temperature field which has been calculated with this intensity distribution using the commercial FEM software ANSYS (Fig. 4 (right)) agrees well with the prescribed temperature profile. This verifies our solution of the inverse heat conduction problem as well as the free-form optic design.

However, in the free-form lens design process, the remaining divergence angle of the incoming beam has been neglected. As the divergence angle of the laser beam is measured to be 2.5 mrad, it is possible to estimate its influence on the obtained intensity distribution. Fig. 5 (left) shows a ray-tracing result for the designed free-form optic with taking into account the remaining divergence angle of the incoming beam. It is clear, that this divergence has a strong influence on the obtained intensity pattern. The sharp edges from Fig. 2 (left) broaden and the overall spot size increases.

It is possible to estimate the effect of the finite divergence angle by calculating the temperature profile if the input intensity is replaced by the intensity from Fig. 5 (left). To do so, we again use the commercial FEM software ANSYS. The result is shown in Fig. 5 (right). It can clearly be seen that the remaining divergence angle consequently results in a broadening of the sharp edges in the temperature field. However, the two temperature steps are still clearly distinguishable and the temperature in the center part is quite homogeneous. As, according to Hawelka, the tolerance for the prescribed temperature-time sequences is rather high, we assume that the achieved temperature profile from Fig. 5 (right) is accurate enough for the functionalization of ZrO_2 coatings.

Alternatively, a different laser beam source with a higher beam quality or a higher total power – to increase the spot size which would diminish the influence of the remaining divergence angle – could be used.

4. Conclusion & Outlook

In this work, we showed how application specific intensity distributions can be used to increase the efficiency of a laser-based functionalization of a wear-protective (nano-)ceramic coating on steel. To do so, we derived a temperature-time sequence that combines the two necessary processing steps – the drying step and the functionalization step. Subsequently, we demonstrated how the application specific intensity distribution can be derived that creates this temperature profile in the workpiece. The obtained intensity

distribution is inhomogeneous and has several very sharp edges. To create this intensity distribution in an experimental setup, we designed a free-form lens and additionally estimated the influence of the finite divergence angle of the laser beam. We verified our approach using the commercial FEM software ANSYS.

In future work, we will use an experimental setup to validate these simulation results.

Acknowledgements

This work was funded by the German Federal Ministry of Education and Research (BMBF) under grant number 13N13476. Furthermore, we thank Rolf Wester (Fraunhofer ILT) for providing the free-form optics design tool.

References

Alifanov, O. M., 1994. Inverse heat transfer problems. Springer, Berlin / Heidelberg.

Bach, F.-W., Möhwald, K., Laarmann, A., Wenz, T., 2005. Moderne Beschichtungsverfahren. WILEY-VCH Verlag GmbH & Co. KGaA, Weinheim.

Bäuerle, A., Bruneton, A., Wester, R., Stollenwerk, J., Loosen, P., 2012. Algorithm for irradiance tailoring using multiple freeform optical surfaces. Optics Express 20, pp. 14477.

Beck, J. V., Blackwell, B., St Clair Jr, C. R., 1985. Inverse heat conduction: ill-posed problems. J. Wiley and Sons, New York.

Bruneton, A., Bäuerle, A., Wester, R., Stollenwerk, J., Loosen, P., 2013. High resolution irradiance tailoring using multiple freeform surfaces. Optics Express 21, pp. 10563.

Dislich, H., 1988. Sol-gel technology for thin films, fibers, preforms, electronics, and specialty shapes, Thin films from the sol-gel process. Noyes Publications.

Hansen, P. C., O'Leary, D. P., 1993. The use of the L-curve in the regularization of discrete ill-posed problems. SIAM Journal of Scientific Computing 14(6), pp. 1487.

Hawelka, D., 2015. Laserbasierte Herstellung nanokeramischer Verschleißschutzschichten auf temperaturempfindlichen Substraten. Apprimus Verlag, Aachen.

Hieke, A., 2000. Diamantähnliche Kohlenstoffschichten (DLC) – verschleißfest und reibarm. Materialwissenschaft und Werkstofftechnik Vol 31, pp. 625.

Mellor, B. G., 2006. Surface coatiings for protection against wear. CRC Press LLC.

Özisik, M. N., Orlande, H. R. B., 2000. Inverse heat transfer. Taylor & Francis, New York.

Spittel, M., Spittel, T., 2009. Metal Forming Data of Ferrous Alloys – deformation behaviour. Springer, Berlin / Heidelberg, pp. 552.

Stollenwerk, J., Holters, M., Wester, R., 2015. Verfahren zur Auslegung einer Anordnung für die Materialbearbeitung eines Werkstücks sowie Anordnung für die Materialbearbeitung eines Werkstücks. German patent DE 102014003483 A1

Uhlmann, I., Hawelka, D., Hildebrandt, E., Pradella, J., Rödel, J., 2013. Structure and mechanical properties of silica doped zirconia thin films. Thin Solid Films 527, pp. 200.

Völl, A., Stollenwerk, J., Loosen, P., 2016. Computing specific intensity distributions for laser material processing by solving an inverse heat conduction problem. Proceedings of SPIE 9741-05.